

See discussions, stats, and author profiles for this publication at: <https://www.researchgate.net/publication/228710780>

High pressure study of structural and electronic properties of calcium chalcogenides

Article in *Journal of Physics Condensed Matter* · July 2005

DOI: 10.1088/0953-8984/17/26/008

CITATIONS

93

READS

364

5 authors, including:



Charifi Zoulikha

Université de M'sila

61 PUBLICATIONS 670 CITATIONS

[SEE PROFILE](#)



H. Baaziz

Université de M'sila

60 PUBLICATIONS 620 CITATIONS

[SEE PROFILE](#)



F. El Haj Hassan

Lebanese University

198 PUBLICATIONS 1,579 CITATIONS

[SEE PROFILE](#)



Nadir Bouarissa

Université de M'sila

294 PUBLICATIONS 2,879 CITATIONS

[SEE PROFILE](#)

Some of the authors of this publication are also working on these related projects:



Quantum well lasers [View project](#)



Low-dimension materials [View project](#)

High pressure study of structural and electronic properties of calcium chalcogenides

Z Charifi¹, H Baaziz¹, F El Haj Hassan^{2,4} and N Bouarissa³

¹ Physics Department, Faculty of Science and Engineering, University of M'sila, 28000 M'sila, Algeria

² Laboratoire de Physique de Matériaux, Faculté des Sciences (I), Université Libanaise, Elhadath, Beirut, Lebanon

³ Physics Department, Faculty of Science, King Khalid University, Abha, PO Box 9004, Saudi Arabia

E-mail: hassan.f@ul.edu.lb

Received 11 April 2005, in final form 17 May 2005

Published 17 June 2005

Online at stacks.iop.org/JPhysCM/17/4083

Abstract

The structural and electronic properties of calcium chalcogenides CaX ($X = \text{S, Se, Te}$) under high pressure have been investigated using the full potential linearized augmented plane wave method within density functional theory. We used both the local density approximation and the generalized gradient approximation (GGA) that is based on exchange–correlation energy optimization for calculating the total energy. Moreover, the Engel–Vosko GGA formalism is applied so as to optimize the corresponding potential for band structure calculations. The equilibrium lattice constant for CaX compounds agrees well with the experimental results. The pressures at which these compounds undergo a structural phase transition from NaCl-type to CsCl-type were calculated. A numerical first-principles calculation of the elastic constants was used to calculate C_{11} , C_{12} and C_{44} . The energy band gaps at ambient conditions in the NaCl-type structure and the volume dependence of band gaps in the CsCl-type structure up to the band overlap metallization were investigated. Besides this, the nature of the chemical bond in these compounds was analysed in terms of electronic charge density.

1. Introduction

The structural phase transformations, as well as metallization under high pressure in alkaline-earth chalcogenides, have attracted considerable interest in the last decade [1]. These compounds form a closed-shell ionic system crystallized in the NaCl-type (B1) structure at

⁴ Author to whom any correspondence should be addressed.

ambient conditions—except for BeO and MgTe (crystallized in the wurtzite structure) and the beryllium chalcogenides (crystallized in the zinc-blende structure).

A noticeable feature in the electronic band structure of the CaX compounds is that there is no d electron in the valence band.

With the application of pressure the NaCl structure of the alkaline-earth chalcogenides undergoes a structural phase transition to CsCl-type (B2) structure with eightfold coordination. CaS, CaSe and CaTe are found to exhibit a structural phase transition with the application of pressures of 40, 38 and 33 GPa, respectively [2]. With the application of further pressure, the metallization occurs in the CsCl structure. The band gaps in these closed-shell insulating materials are expected to decrease as the pressure increases, until finally the empty d-type conduction band drops in energy below the top of the filled p-type valence bands.

Several experimental and theoretical studies of CaX compounds have been published during the last few years. Structural studies of CaS, CaSe and CaTe, under high pressure up to 52 GPa, have been carried out experimentally using x-ray diffraction to observe a first-order phase transformation from the NaCl phase to the CsCl phase [2]. Pressure–volume relationships and structural transitions in CaTe are investigated at high pressure using also x-ray diffraction [3]. The cohesive properties under pressure of CaX compounds have been calculated by using *ab initio* calculations [4]. The elastic constants are investigated using pseudopotential [5] and tight binding theory [6].

Despite these studies a number of basic properties are still unknown, e.g. the pressure behaviour of the band gaps. To understand some of the physical properties of these compounds, a detailed description of electronic structure of these compounds is needed. To the best of our knowledge there are no experimental works exploring the elastic constants and the ionicity factor of CaX compounds, and no calculations based on the full potential linearized augmented plane wave (FP-LAPW) method were performed for any of the CaX compounds. Therefore, the aim of this paper is to provide a comparative study of structural and electronic properties under high pressures, by using the FP-LAPW method, which will complete the existing experimental and theoretical work on CaS, CaSe and CaTe.

To obtain a deeper understanding of elastic properties of these compounds, we need to have a clear idea of the bonding properties. The charge density is an appropriate tool that permits us to better understand the bonding character and the FP-LAPW approach gives an accurate description of the valence charge density. We then correlate this latter quantity with the ionicity factor through an empirical formula [7], which has been successfully applied to other $A^N B^{8-N}$ compounds [8, 9].

The paper is organized as follows: in section 2, we describe the calculation procedure; results and a discussion are presented in section 3; the paper is concluded in section 4.

2. Method of calculations

The calculations are performed using the scalar relativistic FP-LAPW approach as implemented in WIEN2K [10] code within the framework of density functional theory (DFT) [11] that has been shown to yield reliable results for the electronic and structural properties of various solids. For structural properties the exchange–correlation potential was calculated using both the local density approximation (LDA) [12] and also the generalized gradient approximation (GGA) in the form proposed by Perdew *et al* [13]. In addition, and for electronic properties only, we also applied the Engel–Vosko (EVGGA) scheme [14]. In the FP-LAPW method, the wavefunction, charge density and potential are expanded in spherical harmonic functions inside non-overlapping spheres surrounding the atomic sites (muffin-tin spheres) and using a plane wave basis set in the remaining space of the unit cell (interstitial region). A mesh of

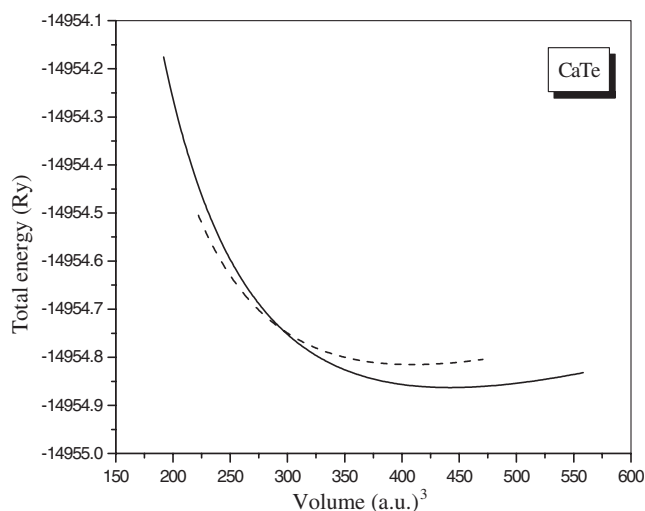


Figure 1. Variation of total energy with unit cell volume in B1 (solid curve) and B2 (dashed curve) structures for CaTe calculated using the GGA.

$7 \times 7 \times 7$ special k -points is taken in the whole Brillouin zone in both B1 and B2 phases. The maximum l quantum number for the wavefunction expansion inside the atomic spheres is confined to $l_{\max} = 10$. The plane wave cut-off of $K_{\max} = 8.0/R_{\text{MT}}$ (R_{MT} is the smallest muffin-tin radius in the unit cell) is chosen for expansion of the wavefunctions in the interstitial region while the charge density is Fourier expanded up to $G_{\text{MAX}} = 14 \text{ Ryd}^{1/2}$. The muffin-tin radius was assumed to be 2, 2.1, 2.3 and 2.4 au for S, Ca, Se and Te, respectively. Both the plane wave cut-off and the number of k -points were varied to ensure total energy convergence.

3. Results and discussion

3.1. Structural properties

CaS, CaSe and CaTe at ambient pressure crystallize in the NaCl structure and undergo a transition to the CsCl structure upon compression. In this work we analyse both structures using the LDA with and without the GGA scheme. The total energies were calculated as a function of volume and as a prototype; the results calculated using the GGA for CaTe are given in figure 1. The curves were obtained by fitting the calculated values to Murnaghan's equation of state [15]. The corresponding equilibrium lattice parameters for both B1 and B2 phases are listed in table 1. It is clearly seen that for all compounds the GGA overestimates the lattice parameter while the LDA underestimates it; these findings are consistent with the general trend of these approximations [16–18].

The cohesive energy is defined as the difference between the energy of an isolated atom and the energy of the same atom in the solid. In order to obtain an accurate value for the cohesive energy, the energy calculations for the isolated atoms and the crystal must be performed at the same level of accuracy. To fulfil such a requirement the energy of an isolated atom was calculated by considering a supercell containing just one atom. The size of this supercell was chosen sufficiently large that the energy convergence with respect to the size of the supercell was less than 0.001 Ryd (large cubic supercells with dimensions of 18 au for S and Ca, 19 au for Te and Se were used). The cohesive energy, the bulk modulus and its pressure derivative

Table 1. Calculated lattice parameter a , bulk modulus B , its pressure derivative B' , cohesive energy E_{coh} and elastic constant parameters at equilibrium volume for NaCl (B1) and CsCl (B2) structures for CaX compounds. The results are compared with the experimental and other theoretical predictions.

| | | Present work | | Experiment | Other theoretical works | | |
|------|----------------------------|--------------|--------|------------|-------------------------|---------------------|--------------------------|
| | | GGA | LDA | [2] | <i>ab initio</i> [4] | Pseudopotential [5] | Tight binding theory [6] |
| CaS | | | | | | | |
| B1 | a (Å) | 5.717 | 5.564 | 5.689 | 5.598 | 5.721 | 5.408 |
| | B (GPa) | 57.42 | 67.40 | 64 | 65.2 | 57 | 115.67 |
| | B' | 3.8 | 4.4 | 4.2 | 4.1 | | |
| | E_{coh} (eV/cell) | -10.4 | -11.4 | | -9.95 | | -12.52 |
| | C_{11} (GPa) | 108.23 | 122.87 | | | 135 | 202.35 |
| | C_{12} (GPa) | 32.01 | 39.66 | | | 20 | 72.42 |
| | C_{44} (GPa) | 36.08 | 41.94 | | | 38 | 67.45 |
| B2 | a (Å) | 3.494 | 3.397 | 3.460 | 3.409 | | |
| | B (GPa) | 60.67 | 77.42 | 64 | 71.2 | | |
| | B' | 3.5 | 5.4 | 4.2 | 4.2 | | |
| | E_{coh} (eV/cell) | -9.6 | -10.8 | | | | |
| | C_{11} (GPa) | 113.60 | 124.44 | | | | |
| | C_{12} (GPa) | 34.20 | 53.91 | | | | |
| | C_{44} (GPa) | 39.01 | 55.90 | | | | |
| CaSe | | | | | | | |
| B1 | a (Å) | 5.968 | 5.790 | 5.916 | 5.829 | 6.087 | 5.71 |
| | B (GPa) | 48.75 | 57.21 | 51 | 56.2 | 50 | 88.92 |
| | B' | 3.4 | 4.4 | 4.2 | 4.1 | | |
| | E_{coh} (eV/cell) | -9.7 | -10.6 | | -8.84 | | -10.17 |
| | C_{11} (GPa) | 95.17 | 106.76 | | | 115 | 155.25 |
| | C_{12} (GPa) | 25.56 | 23.12 | | | 18 | 55.75 |
| | C_{44} (GPa) | 27.11 | 29.90 | | | 31 | 53.51 |
| B2 | a (Å) | 3.653 | 3.550 | 3.611 | 3.559 | | |
| | B (GPa) | 51.41 | 66.35 | 51 | 61.0 | | |
| | B' | 3.8 | 5.4 | 4.2 | 4.2 | | |
| | E_{coh} (eV/cell) | -9.11 | -10.00 | | | | |
| | C_{11} (GPa) | 99.78 | 108.65 | | | | |
| | C_{12} (GPa) | 27.22 | 45.20 | | | | |
| | C_{44} (GPa) | 32.46 | 47.98 | | | | |
| CaTe | | | | | | | |
| B1 | a (Å) | 6.396 | 6.208 | 6.348 | 6.231 | | 6.074 |
| | B (GPa) | 39.60 | 44.03 | 41.8 | 45.4 | | 69.05 |
| | B' | 3.3 | 4.3 | 4.3 | 4.2 | | |
| | E_{coh} (eV/cell) | -9.25 | -10.34 | | -7.61 | | -8.93 |
| | C_{11} (GPa) | 89.26 | 97.42 | | | | 116.96 |
| | C_{12} (GPa) | 14.77 | 17.33 | | | | 45.18 |
| | C_{44} (GPa) | 18.52 | 23.99 | | | | 43.90 |
| B2 | a (Å) | 3.930 | 3.810 | 3.931 | 3.799 | | |
| | B (GPa) | 38.78 | 49.06 | 41.8 | 50 | | |
| | B' | 3.8 | 4.8 | 4.3 | 4.2 | | |
| | E_{coh} (eV/cell) | -8.43 | -9.66 | | | | |
| | C_{11} (GPa) | 93.48 | 111.27 | | | | |
| | C_{12} (GPa) | 14.92 | 17.95 | | | | |
| | C_{44} (GPa) | 20.98 | 26.08 | | | | |

for each compound are compared with available theoretical results in table 1. It is clearly seen that the bulk modulus and the absolute value of the cohesive energy decrease from CaS to CaTe for both phases, i.e. from the lower to the higher atomic number. This suggests that CaTe is more compressible than the other two compounds. It can be noted that Luo *et al* [2] reported identical experimental values of B and B' for the B1 and B2 phase. This may indicate that the available experimental data were not sufficient for a three-parameter fit.

To obtain the elastic constants of these compounds with cubic structure we have used a numerical first-principles calculation by computing the components of the stress tensor ε for small strains, using the method developed recently by Charpin and integrated it in the WIEN2K code [10]. It is well known that a cubic crystal has only three independent elastic constants, C_{11} , C_{12} and C_{44} . Hence, a set of three equations is needed to determine all the constants.

The first equation involves calculating the bulk modulus (B), which is related to the elastic constants, by [19]

$$B = \frac{1}{3}(C_{11} + 2C_{12}). \quad (1)$$

The second one involves applying volume-conserving tetragonal strain:

$$\vec{\varepsilon} = \begin{pmatrix} \varepsilon & 0 & 0 \\ 0 & \varepsilon & 0 \\ 0 & 0 & \frac{1}{1+\varepsilon^2} - 1 \end{pmatrix}. \quad (2)$$

Application of this strain changes the total energy from its initial value as follows:

$$E(\varepsilon) = (C_{11} - C_{12})6V_0\varepsilon^2 + O(\varepsilon^3) \quad (3)$$

where V_0 is the volume of the unit cell.

Finally, for the last type of deformation, we used the volume-conserving rhombohedral strain tensor given by

$$\vec{\varepsilon} = \frac{\varepsilon}{3} \begin{pmatrix} 1 & 1 & 1 \\ 1 & 1 & 1 \\ 1 & 1 & 1 \end{pmatrix} \quad (4)$$

which transform the total energy to

$$E(\varepsilon) = \frac{V_0}{3}(C_{11} + 2C_{12} + 4C_{44})\varepsilon^2 + O(\varepsilon^3). \quad (5)$$

These three equations form the set of equations needed to determine the full elastic tensor. Our LDA and GGA calculated values for the elastic constants are compared with the available results in table 1. It is clearly seen that there is a considerable discrepancy between our results and the theoretical values reported in [6]; however, they are in agreement with the values of [5].

The origin of this discrepancy seems to be the bulk moduli for CaX compounds calculated by the tight binding method in [6] widely exceeding the experimental values. The elastic constant depends on the bulk modulus (equation (1)); hence the significant error in its value leads to the non-valid results for elastic constants. As to the best of our knowledge no experimental value for the elastic constants of these compounds has appeared in the literature, our results for the B2 phase can serve as a prediction for future investigations.

In order to determine the transition pressure at $T = 0$ K, the enthalpy, $H = E_0 + PV$, should be calculated [20]. The stable structure at a given pressure is the state for which the enthalpy has its lowest value. Hence the common tangent to the curves in figure 1 indicates the phase transition pressure. Following such a procedure the rock-salt to CsCl transition pressures were calculated using the LDA with and without the GGA scheme. The calculated values for the transition pressures and the transition volumes are given in table 2.

Table 2. Calculated values of the transition pressure P_t and transition volumes $V_t(\text{B1})/V_0$ for CaX compounds. The results are compared with the experimental and other theoretical predictions (V_0 is the experimental equilibrium volume for the B1 phase).

| | | Present work | | Expt | Other theoretical works |
|------|----------------------|--------------|-------|-------------------|-------------------------|
| | | GGA | LDA | | [4] |
| CaS | P_t (GPa) | 37.22 | 35.39 | 40 [2] | 45 |
| | $V_t(\text{B1})/V_0$ | 0.72 | 0.71 | 0.73 [2] | 0.71 |
| CaSe | P_t (GPa) | 34.38 | 40.65 | 38 [2] | 45 |
| | $V_t(\text{B1})/V_0$ | 0.74 | 0.68 | 0.70 [2] | 0.69 |
| CaTe | P_t (GPa) | 30.41 | 31.58 | 33 [2] 35 [3] | 27 |
| | $V_t(\text{B1})/V_0$ | 0.72 | 0.68 | 0.74 [2] 0.70 [3] | 0.73 |

Table 3. The band gap calculated within different approximations in the NaCl (B1) and CsCl (B2) structures for CaX compounds (all values are given in eV).

| | | B1 phase | | B2 phase | |
|------|--|----------|-------|----------|-------|
| | | GGA | EVGGA | GGA | EVGGA |
| CaS | | 2.39 | 3.18 | 1.35 | 2.06 |
| CaSe | | 2.10 | 2.81 | 0.79 | 1.49 |
| CaTe | | 1.57 | 2.23 | 0.00728 | 0.55 |

3.2. Electronic properties

The self-consistent scalar relativistic band structures of CaS, CaSe and CaTe were obtained in the B1 and B2 phases at equilibrium volume as well as at high pressure within the GGA and EV-GGA schemes.

It is well known that the LDA and the GGA usually underestimate the energy gap [21, 22]. This is mainly due to the fact that they have simple forms that are not sufficiently flexible for accurately reproducing both exchange–correlation energy and its charge derivative. Engel and Vosko by considering this shortcoming constructed a new functional form of the GGA which was able to better reproduce the exchange potential at the expense of less agreement as regards exchange energy. This approach, which is called the EVGGA, yields a better band splitting and some other properties which mainly depend on the accuracy of the exchange–correlation potential. On the other hand, in this method, the quantities which depend on an accurate description of the exchange energy E_x such as equilibrium volumes and the bulk modulus, are in poor agreement with experiment. The band structure calculated using the GGA and the EV-GGA for CaSe and CaTe were similar except for the value of their band gap which was higher within the EVGGA. Because of this similarity, only the band structures of CaTe for both phases B1 and B2, calculated within the EVGGA, are presented in figure 2.

In the case of the B1 structure, our study yields an indirect band gap ($\Gamma \rightarrow X$). The lowest lying band shown in the graph arises mainly from the chalcogenide valence s states. The upper valence bands that lie above this band are due to p states with the top occurring at the Γ point. The conduction band arises mainly from the Ca d state with the minimum energy occurring at X points. The calculated values of the band gap for each compound are given in table 3.

We also studied the electronic properties of CaX compounds in the B2 phase at equilibrium volume which show a direct band gap ($M \rightarrow M$) except for CaS using the EVGGA, which predicted a conduction band minimum located along the Γ direction. No experimental work

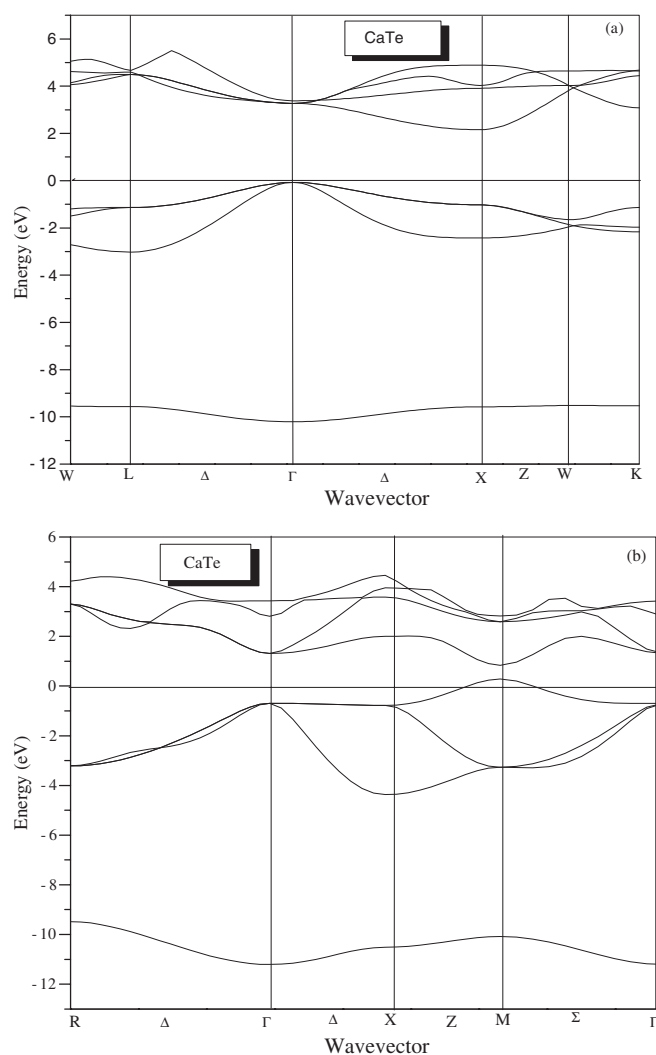


Figure 2. Band structure of CaTe obtained using the EVGGA scheme calculated along high symmetry directions for (a) NaCl (B1) structure and (b) CsCl (B2) structure.

for the band gap under pressure has been reported for these compounds; hence more optical measurement are required to confirm our results.

With the application of further pressure, band overlap metallization occurs. The metallization is described as due to band broadening with the increase in pressure and subsequent overlap of the filled valence band (the p-like valence band of the chalcogen atom) and the conduction band (the d-like conduction band of the cation) [23]. The volume dependence of the band gaps in the CsCl structure is shown in figure 3. The volume and pressures at which the band gap becomes zero are given in table 4.

The bonding nature of the solids can be described accurately by using electronic density plots [24, 25], that have been calculated in the context of the first-principles approach. The charge density in our calculation is derived from a highly converged wavefunction; hence the result is very reliable and it can then be used to study the bonding nature of the solid.

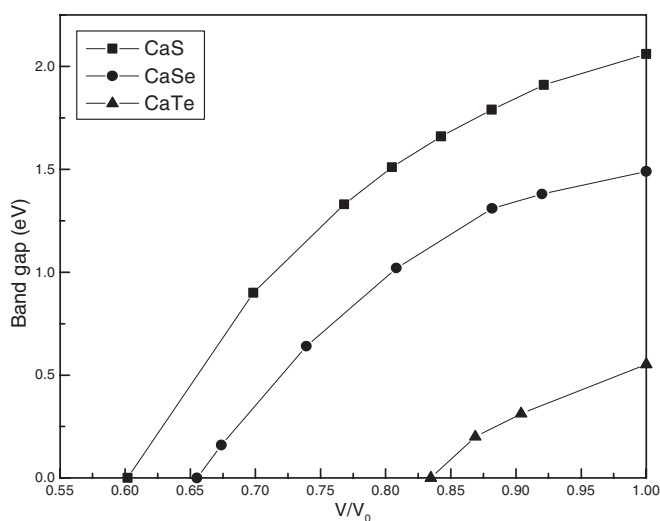


Figure 3. Volume dependence of band gaps for CaS, CaSe and CaTe in the B2 phase using the EVGGA scheme.

Table 4. Transition pressures and transition volume for metallization transformation in CaS, CaSe and CaTe calculated with the EVGGA scheme.

| | V_m/V_0 | Pressure (GPa) |
|------|-----------|----------------|
| CaS | 0.602 | 85.07 |
| CaSe | 0.655 | 54.01 |
| CaTe | 0.834 | 39.87 |

To obtain an estimated value of the ionicity factor for CaS, CaSe and CaTe compounds, we have used an empirical formula [7]. In this approach, the total area occupied by the valence charge density is divided into two parts with respect to the centre. S_C and S_A are the areas of the cation and anion sides, respectively, and the ionicity factor is defined as

$$f_i = \left(\frac{S_A}{S_A + \lambda S_C} \right)^\lambda \quad (6)$$

where λ is a parameter separating the highly ionic elements from the weakly ionic ones. $\lambda = -1$ for elemental and III–V semiconductors; $\lambda = +1$ for II–VI and I–VII semiconductors.

Following such an approach, we have calculated the ionicity values for CaS, CaSe and CaTe; the results are summarized in table 5. The density profile of CaTe is shown in figure 4. Our values calculated within the GGA agree well with the Phillips results [26] and they decrease when the group VI anion changes from S to Te. Our results suggest the following ionicity order: CaS > CaSe > CaTe.

4. Concluding remarks

We have applied a FP-LAPW method to study the structural and electronic properties of CaS, CaSe and CaTe compounds. A summary of the key findings follows.

- (i) Our GGA calculated values for the pressures of the transition from B1 to B2 phases are in agreement with the available experimental results.

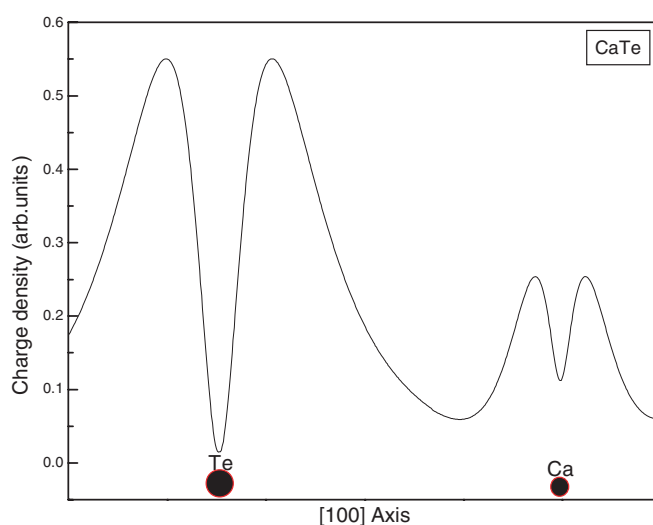


Figure 4. The profile of the total valence charge densities for CaTe calculated within the GGA at equilibrium volume in the B1 phase along the [1 0 0] direction.

(This figure is in colour only in the electronic version)

Table 5. Calculated ionicity values of CaX compounds for both B1 and B2 phases at equilibrium volume.

| | f_i (B1) | | f_i (B2) | | f_i (B1) Phillips [26] |
|------|------------|-------|------------|-------|-----------------------------|
| | GGA | LDA | GGA | LDA | |
| CaS | 0.892 | 0.852 | 0.884 | 0.833 | 0.902 |
| CaSe | 0.874 | 0.824 | 0.863 | 0.801 | 0.900 |
| CaTe | 0.859 | 0.797 | 0.841 | 0.790 | 0.894 |

- (ii) The lattice parameters that we calculated using the GGA scheme are in better agreement with the experiment as compared to previous theoretical predictions. The bulk modulus and the cohesive energies values in both B1 and B2 phases suggest that BaTe is more compressible than the other two compounds.
- (iii) A numerical first-principles method was used to calculate the elastic constants C_{11} , C_{12} and C_{44} which have not yet been established experimentally. There is a considerable discrepancy between our results and those calculated using tight binding theory. The origin of this disagreement is the significant overestimation of the bulk modulus calculated by the tight binding method. Our results for elastic constants in the B2 phase can serve as a prediction for future investigations.
- (iv) The energy band gaps at ambient conditions in the NaCl-type structure and the volume dependence of band gaps in the CsCl-type structure were calculated. The pressure and the volumes at which band overlap metallization occurs were also obtained.
- (v) The bonding character has been discussed in terms of the charge density and shows a strong localization of the charge around the anion side. This behaviour is generally common in semiconductors. Furthermore, the ionicity factor is found to compare well with the Phillips ionicity scale.

References

- [1] Ruoff A L and Grzybowski T A 1985 *Solid State Physics Under Pressure* ed S Minomura (Tokyo: Terra Scientific)
- [2] Luo H, Greene R G, Handehari K G, Li T and Ruoff A L 1994 *Phys. Rev. B* **50** 16232
- [3] Zimmer H G, Winzen H and Sayassen K 1985 *Phys. Rev. B* **32** 4066
- [4] Cortona P and Masri P 1998 *J. Phys.: Condens. Matter* **10** 8947
- [5] Marinelli F and Lichanot A 2003 *Chem. Phys. Lett.* **367** 430
- [6] Straub G K and Harrison W A 1989 *Phys. Rev. B* **39** 10325
- [7] Zaoui A, Ferhat M, Khelifa B, Dufour J P and Aourag H 1994 *Phys. Status Solidi b* **185** 163
- [8] El Haj Hassan F, Zaoui A and Sekkal W 2001 *Mater. Sci. Eng. B* **87** 40
- [9] El Haj Hassan F, Akbarzadeh H and Zoaeter M 2004 *J. Phys.: Condens. Matter* **16** 293
- [10] Blaha P, Schwarz K, Madsen G K H, Kvasnicka D and Luitz J 2001 *WIEN2K, an Augmented Plane Wave + Local Orbitals Program for Calculating Crystal Properties* Karlheinz Schwarz, Techn. Universitat, Wien, Austria (ISBN 3-9501031-1-2)
- [11] Hohenberg P and Kohn W 1964 *Phys. Rev. B* **136** 864
- [12] Kohn W and Sham L J 1965 *Phys. Rev. A* **140** 1133
- [13] Perdew J P, Burke S and Ernzerhof M 1996 *Phys. Rev. Lett.* **77** 3865
- [14] Engel E and Vosko S H 1993 *Phys. Rev. B* **47** 13164
- [15] Murnaghan F D 1944 *Proc. Natl Acad. Sci. USA* **30** 5390
- [16] Mokhtari A and Akbarzadeh H 2002 *Physica B* **324** 305
- [17] El Haj Hassan F, Akbarzadeh H, Hashemifar S J and Mokhtari A 2004 *J. Phys. Chem. Solids* **65** 1871
- [18] El Haj Hassan F, Akbarzadeh H and Hashemifar S J 2004 *J. Phys.: Condens. Matter* **16** 3329
- [19] Schreiber E, Anderson O L and Soga N 1973 *Elastic Constants and their Measurement* (New York: McGraw-Hill)
- [20] Wettling W and Windscheif J 1984 *Solid State Commun.* **50** 33
- [21] Dufek P, Blaha P and Schwarz K 1994 *Phys. Rev. B* **50** 7279
- [22] Bachelet G B and Christensen N E 1985 *Phys. Rev. B* **31** 879
- [23] Ross M and McMahan A K 1981 *Physics of Solids Under High Pressures* ed J S Schilling and R N Shelton (New York: North-Holland)
- [24] Hoffman R 1988 *Rev. Mod. Phys.* **60** 801
- [25] Gellatt C D Jr, Williams A R and Moruzzi V L 1983 *Phys. Rev. B* **27** 2005
- [26] Phillips J C 1970 *Rev. Mod. Phys.* **42** 317